ARTICLE
Journal of Cellular Biochemistry 9999:1–8 (2017)

Journal of Cellular Biochemistry

Liposomes as a Putative Tool to Investigate NAADP Signaling in Vasculogenesis

Francesca Di Nezza,[1] Estella Zuccolo,[2] Valentina Poletto,[3] Vittorio Rosti,[3] Antonio De Luca,[4] Francesco Moccia,[2] Germano Guerra,[5] and Luigi Ambrosone[5]*

[1]*Department of Bioscience and Territory (DIBT), University of Molise, Contrada Lappone Pesche, Isernia 86090, Italy*

[2]*Laboratory of General Physiology, Department of Biology and Biotechnology "L. Spallanzani", University of Pavia, Pavia 27100, Italy*

[3]*Biotechnology Research Laboratory, Center for the Study of Myelofibrosis, Fondazione IRCCS Policlinico San Matteo, Pavia 27100, Italy*

[4]*Department of Mental and Physical Health and Preventive Medicine, Section of Human Anatomy, Università degli Studi della Campania "L. Vanvitelli", Naples 80138, Italy*

[5]*Department of Medicine and Health Sciences "Vincenzo Tiberio", Centre of Nanomedicine, University of Molise, Campobasso 86100, Italy*

ABSTRACT

Nicotinic acid adenine dinucleotide phosphate (NAADP) is the newest discovered intracellular second messengers, which is able to release Ca^{2+} stored within endolysosomal (EL) vesicles. NAADP-induced Ca^{2+} signals mediate a growing number of cellular functions, ranging from proliferation to muscle contraction and differentiation. Recently, NAADP has recently been shown to regulate angiogenesis by promoting endothelial cell growth. It is, however, still unknown whether NAADP stimulates proliferation also in endothelial progenitor cells, which are mobilized in circulation after an ischemic insult to induce tissue revascularization. Herein, we described a novel approach to prepare NAADP-containing liposomes, which are highly cell membrane permeable and are therefore amenable for stimulating cell activity. Accordingly, NAADP-containing liposomes evoked an increase in intracellular Ca^{2+} concentration, which was inhibited by NED-19, a selective inhibitor of NAADP-induced Ca^{2+} release. Furthermore, NAADP-containing liposomes promoted EPC proliferation, a process which was inhibited by NED-19 and BAPTA, a membrane permeable intracellular Ca^{2+} buffer. Therefore, NAADP-containing liposomes stand out as a promising tool to promote revascularization of hypoxic/ischemic tissues by favoring EPC proliferation. J. Cell. Biochem. 9999: 1–8, 2017.

KEY WORDS: LIPOSOMES; NAADP; Ca^{2+} SIGNALING; ENDOTHELIAL PROGENITOR CELLS; VASCULOGENESIS

Nicotinic acid adenine dinucleotide phosphate (NAADP) has been established as a Ca^{2+} releasing intracellular second messenger in a growing number of cell types [Morgan et al., 2011; Galione, 2015]. NAADP triggers endogenous Ca^{2+} mobilization by targeting two-pore channels, TPC1 and TPC2, which localize to the acidic Ca^{2+} stores of the endolysosomal system (EL) [Morgan et al., 2011]. Local NAADP-evoked Ca^{2+} signals may in turn be amplified into a global Ca^{2+} wave by the recruitment of either ryanodine or inositol-1,4,5-trisphosphate receptors on the adjacent membranes of the endoplasmic reticulum (ER) [Galione, 2015; Penny et al., 2015; Ronco et al., 2015]. Alternatively, NAADP could directly activate type 1 RyRs, as demonstrated in murine T cells [Wolf et al., 2015], or gate a Ca^{2+}-permeable current on the plasma membrane, as shown in starfish oocytes [Moccia et al., 2003]. NAADP may thus control a multitude of Ca^{2+}-dependent cellular events, such as fertilization, differentiation, cardiac contractility, skeletal muscle differentiation, glucose secretion, and T-cell receptor (TCR) signaling [Johnson and Misler, 2002; Moccia et al., 2006; Morgan et al., 2011; Galione, 2015; Wolf et al., 2015]. Recent work showed that NAADP-evoked Ca^{2+} signals stimulated angiogenesis in vitro and neovascularization in vivo [Favia et al., 2014]. A subsequent report revealed that a functional EL Ca^{2+} store is also present in human endothelial progenitor cells (hEPCs) [Zuccolo et al., 2015], which are mobilized from bone marrow to restore the vascular network and rescue local

Francesco Mocciab, Germano Guerrae, and Luigi Ambrosonee shared senior authorship.

*Correspondence to: Prof. Luigi Ambrone, Department of Medicine and Health Sciences "Vincenzo Tiberio," Centre for Nanomedicine, University of Molise, Campobasso 86100, Italy. E-mail: ambroson@unimol.it

Manuscript Received: 3 April 2017; Manuscript Accepted: 3 April 2017

Accepted manuscript online in Wiley Online Library (wileyonlinelibrary.com): 04 April 2017

DOI 10.1002/jcb.26019 • © 2017 Wiley Periodicals, Inc.

blood perfusion in ischemic tissues, according to a process termed vasculogenesis [Basile and Yoder, 2014; Moccia et al., 2015]. An increase in intracellular Ca^{2+} concentration ($[Ca^{2+}]_i$) has been put forward as an alternative tool to improve the therapeutic outcome of regenerative medicine in ischemic patients [Ferreira-Martins et al., 2009; Gwathmey et al., 2011; Moccia et al., 2015]. A major problem in assessing the pro-angiogenic effect of NAADP and exploiting its therapeutic potential is that, just like all known second messengers, NAADP is electrically charged to prevent its leakage from the cells and is, therefore, membrane-impermeant. Several approaches have been developed to intracellularly deliver NAADP, including intracellular dialysis through a patch-clamp pipette [Cancela et al., 2003; Ronco et al., 2015] and intracellular microinjection [Johnson and Misler, 2002]. However, these approaches are technically challenging, require the analysis of hundreds of single cells and, in the case of microinjection, may cause a permanent damage to the cell. To overcome these hurdles, Churchill and coworkers synthesized an acetoxymethyl ester of NAADP (NAADP-AM), which is cell-permeant, is taken up into the cells and has been used by this group to investigate the outcome of NAADP-induced Ca^{2+} mobilization in different cellular models [Parkesh et al., 2008; Galione et al., 2014]. Herein, we developed a nanocarrier with the capability of encasing and releasing NAADP. The challenge was to load the second messenger into liposomal nanocarriers without disruption/changes of vesicle shape and, at the same time, permitting NAADP to permeate the cell membrane. We demonstrated that liposome-introduced NAADP caused a dose-dependent increase in $[Ca^{2+}]_i$ in hEPCs. NAADP-evoked Ca^{2+} signals were sensitive to NED-19, a TPC inhibitor, which confirmed the activation of the EL Ca^{2+} store. Moreover, NAADP-containing liposomes promoted hEPC proliferation in a Ca^{2+}-dependent manner. It turns out that the liposomal delivery of NAADP stands out as a promising technique to selectively promote post-ischemic neovascularization in injured tissues.

MATERIALS AND METHODS

CHEMICALS

Phosphate buffered saline (PBS) was from Sigma. Soybean lecithin epikuron 130 P (EPK130) was obtained from Cargill Food Ingredient Gmb. According to the manufacturer, EPK130 was a 65% wt/wt mixture of natural phospholipids with the following distribution of headpolar groups: phosphatidylcholine (PC, 3,033%), phosphatidyl-ethanolamine (PE, 1,215%), phosphatidylinositol (PI, 1,316%), and phosphatidic acid (PA, 36%). Fatty acids were mainly polyunsaturated (3,134%) with minor fractions of saturated (1,113%) and monounsaturated (36%). EBM and EGM-2 MV Bullet Kit were purchased from Clonetics (Cell System, St. Katharinen, Germany). Fura-2/AM was obtained from Molecular Probes (Molecular Probes Europe BV, Leiden, the Netherlands). All other chemicals were obtained from Sigma Chemical Co. (St. Louis, MO).

LIPOSOME PREPARATION

Liposomes were prepared from lecithin by a thin film hydration method. A thin film was formed by dissolving the lecithin in chloroform/methanol solution (2:1, v/v) in a round bottom flask and following removal of the solvent under vacuum condition at room temperature, which ensured complete removal of the solvents. The film was then hydrated with PBS buffer (10 mM, pH 7.4) to make a 20 mL of lipid coarse dispersion. Liposomes were prepared by adding cholesterol in a 89:20 lecithin:cholesterol molar ratio, codissolved in chloroform and then dried. The dried film from a flask was suspended in 4 mL of rehydration solution. The resulting liposomal dispersion was sonicated [Bufalo et al., 2017] for 3 min (Ultrasound Homogenizer-Biologics) and extruded 21 times with 100 nm filter. Finally, the mixture was dialyzed in PBS bulk for 24 h with three bulk-changes. Properties of liposomes were modulated by varying the rehydration solution composition.

A first liposome type was generated with a PBS solution containing 70 g of NAADP and 0.042 mg of KCl, it is referred as K-liposome (KL). A second liposome type was prepared from PBS solution containing only 70 g of NAADP referred as P-liposome (PL). Moreover, liposomes free to NAADP and KCl, were prepared directly from the PBS solution, this type of liposome referred as FL was used as reference.

SIZE AND ζ-POTENTIAL MEASUREMENTS

Liposomes size was measured by a dynamic light scattering particle size analyzer which has a measuring range from 0.6 nm to 6 m (Zetasizer Nano ZS90, Malvern Instruments Ltd., Worcester-shire, UK). Dynamic light scattering, also known as PCS (Photon Correlation Spectroscopy), measures Brownian motion and relates this to the size of the particles [Lopez et al., 2004]. It does this by illuminating the particles with a laser and analyzing the intensity fluctuations in the scattered light. The relationship between the size of a particle and its speed due to Brownian motion is defined by the Stokes–Einstein equation [Ambrosone et al., 1999]. The final particle diameter was calculated from a mean of at least three measurements. The ζ-potential was measured using the Zetasizer Nano Z S90 which measures the distribution of the electrophoretic mobility of particles with a size range from 3 nm to 10 m using the laser Doppler velocity technique.

SCANNING ELECTRON MICROSCOPY

Scanning electron micrographs were obtained using the specific malachite green fixation technique described elsewhere [Ishi et al., 1995; Aihua et al., 2003]. Briefly, pieces of qualitative filter paper (Whatman 2) were immersed in the lipid vesicles suspension and then removed rapidly. Lipid vesicles adsorbed on the filter paper were fixed by immersion for 24 h at 4°C in 1% (v/v) glutaraldehyde and 1% (w/v) malachite green mixed buffer solution (NaH2PO4–Na2HPO4, pH 7.4). After fixation the lipid vesicles were briefly washed in buffer solution and reacted for 8 h with cold 1% (w/v) osmium tetroxide buffered with phosphate. All samples were subsequently dehydrated in a graded ethanol series. After critical point drying with critical carbon dioxide, the fixed lipid vesicles were mounted on a sample stage with double-sided adhesive tape, vacuum.

ISOLATION AND CULTIVATION OF ENDOTHELIAL COLONY FORMING CELLS

Among the many EPC subtypes described in Literature [Basile and Yoder, 2014], we focused on endothelial colony forming cells

(ECFCs), which represent the only EPC population truly belonging to the endothelial phenotype. As described elsewhere [Moccia et al., 2017; Zuccolo et al., 2016b], blood samples (40 mL) were obtained from healthy human volunteers aged from 22 to 32 years old ($n = 12$). The Institutional Review Boards at Istituto di Ricovero e Cura a Carattere Scientifico Policlinico San Matteo Foundation in Pavia approved all protocols and specifically approved this study. Informed written consent was obtained according to the Declaration of Helsinki. Mononuclear cells (MNCs) were separated from peripheral blood (PB) by density gradient centrifugation on lymphocyte separation medium for 30 min at 400*g* and washed twice in EBM-2 with 2% FCS. A median of 36×10^6 MNCs (range 18–66) were plated on collagen-coated culture dishes (BD Biosciences) in the presence of the endothelial cell growth medium EGM-2 MV Bullet Kit (Lonza) containing endothelial basal medium (EBM-2), 5% foetal bovine serum (FBS), recombinant human (rh) EGF, rhVEGF, rhFGF-B, rhIGF-1, ascorbic acid and heparin, and maintained at 37°C in 5% CO_2 and humidified atmosphere. Discard of non-adherent cells was performed after 2 days; thereafter medium was changed three times a week. The outgrowth of endothelial cells from adherent MNCs was characterized by the formation of a cluster of cobblestone-appearing cells. That ECFCs-derived colonies belonged to endothelial lineage was confirmed as described in [Moccia et al., 2017]. As already shown in [Moccia et al., 2017], the immunophenotype of ECFCs does not change at different passages in culture.

INTRACELLULAR Ca^{2+} MEASUREMENTS

Intracellular Ca^{2+} signals were measured as previously described [Zuccolo et al., 2016a,b]. ECFCs were loaded with 4 μM Fura-2 acetoxymethyl ester (Fura-2/AM; 1 mM stock in dimethyl sulfoxide) in physiological salt solution (PSS) for 30 min at room temperature. PSS had the following composition (in mM): 150 NaCl, 6 KCl, 1.5 CaCl2, 1 MgCl2, 10 Glucose, 10 Hepes. The solution was then titrated to pH 7.4 with NaOH and its osmolality, as measured with an osmometer (Wescor 5500, Logan, UT), was 300–310 mmol/kg. After washing in PSS, the coverslip was fixed to the bottom of a Petri dish and the cells observed by an upright epifluorescence Axiolab microscope (Carl Zeiss, Oberkochen, Germany), usually equipped with a Zeiss 40 Achroplan objective (water-immersion, 2.0 mm working distance, 0.9 numerical aperture). ECFCs were excited alternately at 340 and 380 nm, and the emitted light was detected at 510 nm. A first neutral density filter (1 or 0.3 optical density) reduced the overall intensity of the excitation light and a second neutral density filter (optical density = 0.3) was coupled to the 380 nm filter to approach the intensity of the 340 nm light. A round diaphragm was used to increase the contrast. The excitation filters were mounted on a filter wheel (Lambda 10, Sutter Instrument, Novato, CA). Custom software, working in the LINUX environment, was used to drive the camera (Extended-ISIS Camera, Photonic Science, Millham, UK) and the filter wheel, and to measure and plot on-line the fluorescence from 1,015 rectangular regions of interest (ROI) enclosing 1,015 single cells. Each ROI was identified by a number. Since cell borders were not clearly identifiable, a ROI may not include the whole EPC or may include part of an adjacent ECFC. Adjacent ROIs never superimposed. The $[Ca^{2+}]_i$ was monitored by measuring, for each ROI, the ratio of the mean fluorescence emitted at 510 nm when exciting alternatively at 340 and 380 nm (shortly termed ratio). An increase in $[Ca^{2+}]_i$ causes an increase in the ratio [Zuccolo et al., 2016a,b]. Ratio measurements were performed and plotted on-line every 3 s. The experiments were performed at room temperature (22°C).

PROLIFERATION ASSAYS

As described elsewhere [Dragoni et al., 2015; Zuccolo et al., 2016b], the proliferative effect of NAADP was evaluated by plating a total of 1×10^5 ECFCs-derived cells (first passage) in 30-mm collagen-treated dishes in the presence of: (1) EBM-2 + 5% FBS; (2) 5% FBS + EGM-2; (3) 5% FBS + EGM-2 + PL (1:30); and (4) 5% FBS + EGM-2 + KL (1:30). Cultures were incubated at 37°C (in 5% CO_2 and humidified atmosphere) and cell growth assessed every day until confluence was reached in control cultures. At this point, cells were recovered by trypsinization from all dishes and the cell number assessed by counting in a haemocytometer. In order to assess the impact of Ca^{2+} signaling on NAADP-promoted ECFC proliferation, cells were seeded in the presence of EGM-2 + 20 μM AA supplemented with (1) 5% FBS + EGM-2 + PL (1:30) + BAPTA (30 μM, 30 min pre-incubation); (2) 5% FBS + EGM-2 + PL (1:30) + Ned-19 (10 μM, 30 min pre-incubation). Preliminary experiments showed no unspecific or toxic effect for each agent when used at these concentrations. Each assay was repeated in triplicate.

RESULTS

LIPOSOME CHARACTERIZATION

NAADP is a dinucleotide that only differs from the house-keeping enzyme cofactor, NADP by a hydroxyl group and yet this minor modification converts it into the most potent Ca^{2+}-mobilizing second messenger. As one can see in Figure 1, the negative charge on a molecular surface is due to the presence of highly polarized phosphate groups. Such negative charge triggers strong repulsive interactions between NAADP molecules and membrane cell. In order to obtain an efficient shielding of the repulsive forces, various liposomes were prepared. The chemical and physical characteristics of liposome-containing nanocarriers were assessed by measuring the particle size (D), polidispersity index (PDI), and ζ-potential (Zp) at 25, 30, 37, 40, and 45°C, for each liposome type. The results are summarized in Figure 2. As it can be seen, KLs exhibit a hydrodynamic radius (55 nm) considerably smaller than reference FLs. In contrast, PLs have a size substantially equal to the reference, although it tends to increase at high temperatures, oscillating in the range 65–70 nm. Correspondingly, PDI values are 0.22 and 0.32 for KLs and PLs which are both larger than the reference (0.15 nm) (Fig. 3) and remain practically constant in the entire temperature range. Formation and accumulation of polar hydrolysis products in the membrane reflect in changes of hydrogen bonding interaction [Ambrosone et al., 1999; Lopez et al., 2004; Di Biasio et al., 2009]. One may expected that Zp of liposome should be also sensitive to the NAADP action. Figure 2 shows that Zp for KLs is slightly more negative than PLs, so that, on the basis of physico–chemical parameters measured, one at first

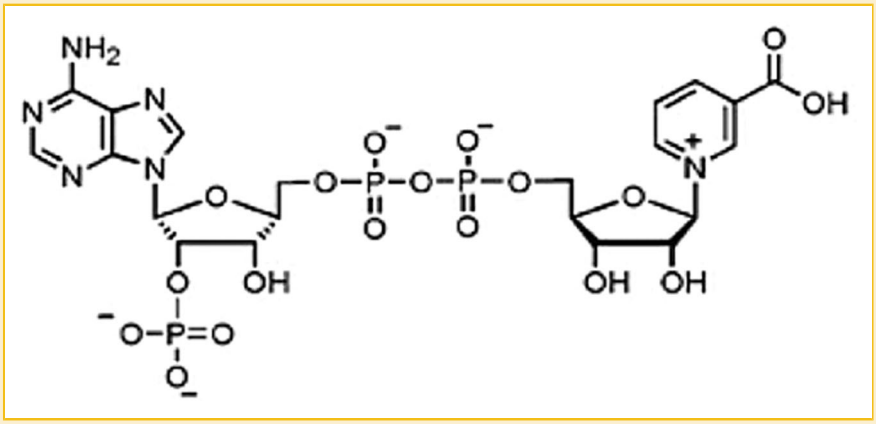

Fig. 1. Molecular structure of NAADP.

glance one might be tempted to conclude that KLs should be excellent carriers for NAADP [Brailoiu et al., 2003, 2005]. A more careful examination, however, reveals that this conclusion is not justified because a large negative charge on a smaller liposome increases its surface charge and renders it impermeable to the cell membrane.

NAADP CONTAINING LIPOSOMES INCREASE $[Ca^{2+}]_i$ IN ECFCs

In order to assess whether NAADP-loaded liposomes are able to cause an increase in $[Ca^{2+}]_i$, we performed Ca^{2+} imaging experiments in Fura-2/AM-loaded ECFCs. After a short recording in PSS, external Ca^{2+} was removed to exclusively focus on Ca^{2+} released from the EL system. The following dilutions were probed for both KLs and PLs: 1:20, 1:25, and 1:30. Figure 4A shows that, for each dilution, KL dispersions failed to increase $[Ca^{2+}]_i$. This finding reinforces the notion that the surface charge has a crucial role in permitting liposomes to be internalized into the cell. Accordingly, PL dispersions increased $[Ca^{2+}]_i$ at each dilution (Fig. 4B), while empty liposomes did not alter intracellular Ca^{2+} levels (not shown). As a control, PLs not filled with NAADP did not increase $[Ca^{2+}]_i$ (Fig. 4B). While the percentage of responding ECFCs was significantly ($P < 0.05$) higher at 1:30 (Fig. 4C), the magnitude of the Ca^{2+} response was greater at 1:20 (Fig. 4D). The involvement of NAADP receptors, that in ECFCs are represented only by TPC1 [Zuccolo et al., 2016b], was probed with NED-19, a specific blocker of NAADP-induced Ca^{2+} release [Morgan et al., 2011; Ronco et al., 2015]. NED-19 (10 μM, 30 min) fully

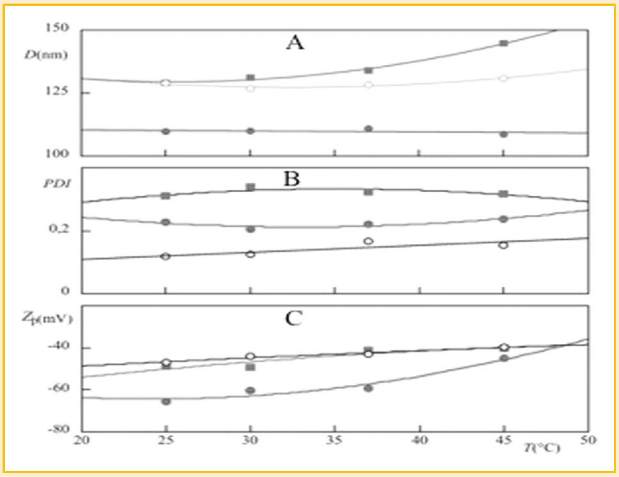

Fig. 2. Chemical and physical characteristics of nanocarriers based Epikuron 130P. Liposomes containing NAADP prepared in PBS (gray squares) and PBS–KCl (grey squares) are compared with liposomes prepared in PBS solution, but empty (white circles). (A) Droplet size, (B) Polydispersity index (PDI), (C) Z-potential (Z_p) are monitored as a temperature function. The lines are guides for the eyes.

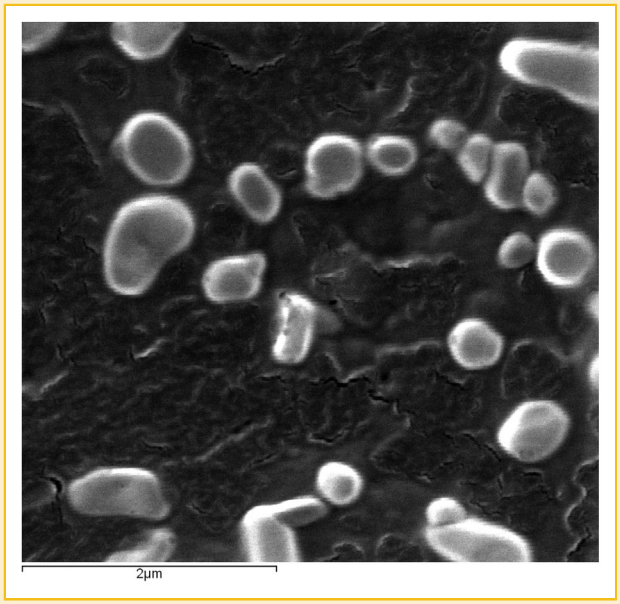

Fig. 3. Scanning electron microscopy of NAADP-filled liposomes. Scanning electron micrograph of lipid vesicles fixed using the malachite green technique.

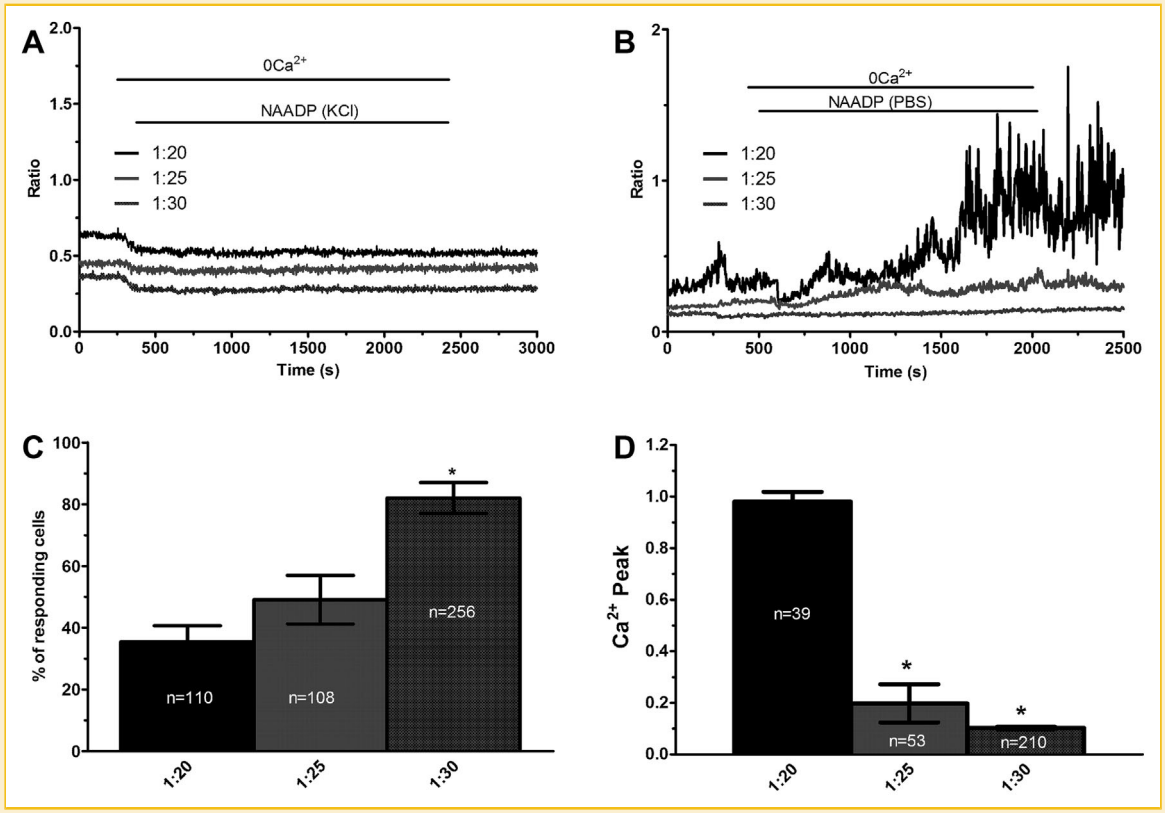

Fig. 4. Liposome-introduced NAADP increase the $[Ca^{2+}]_i$ in ECFCs. (A) KL dispersions do not increase $[Ca^{2+}]_i$ in ECFCs. (B) PL dispersions cause a robust increase in $[Ca^{2+}]_i$ in ECFCs when administered at both 1:20 (A) or 1:30 (B) dilution. Mean ± SE of the percentage of responding cells (C) and of the magnitude (D) of NAADP-evoked Ca^{2+} signals have been reported as bar histograms. The asterisk indicates *t*-test *P*-value <0.05. The amplitude of the Ca^{2+} response to the 1:20 dilution is remarkable smaller than that induced by 1:30 dilution and cannot be appreciated with this Y-ordinate scale.

prevented the Ca^{2+} response to NAADP (Fig. 5), thereby confirming that NAADP delivered through extracellular PLs was acting at its established intracellular target.

NAADP-CONTAINING LIPOSOMES STIMULATE ECFC PROLIFERATION

It has now been recognized that an increase in $[Ca^{2+}]_i$ plays a key role in inducing hECFC proliferation [Moccia et al., 2014; Moccia and Guerra, 2016]. In order to assess whether liposome-introduced NAADP has the potential to be exploited for regenerative purposes, we assessed whether it induces proliferation in ECFCs. As shown in Figure 6, KLs (1:20) failed to induce ECFC proliferation, while PLs (1:20) caused a significant ($P < 0.05$) increase in the rate of ECFC growth. Importantly, liposomes-elicited ECFC proliferation was inhibited by BAPTA (30 μM, 30 min), a membrane-permeable buffer of intracellular Ca^{2+} levels, and NED-19 (10 μM, 30 min). These results provide the first evidence that exogenously administrated NAADP stimulates ECFC growth and suggest that NAADP-containing PL dispersions could be successfully exploited to accelerate revascularization in ischemic diseases. Thus, our results indicate that it is possible to load the liposomes with NAADP and modulate their surface charge to make them efficient nanocarriers.

DISCUSSION

Liposomes are widely employed as an effective drug delivery platform to target endothelium and promote the reconstruction of the vascular network in tissues damaged by an ischemic insult, such as myocardial infarction [Dasa et al., 2015] and ischemic stroke [Liu et al., 2011]. Recently, the induction of spatio-temporally coordinated intracellular Ca^{2+} signals in progenitor cells belonging either to the endothelial [Moccia et al., 2015] or cardiac [Ferreira-Martins et al., 2009] lineage has been proposed as an alternative tool to induce revascularization of the ischemic heart. Of note, ECFCs, the hEPC subset employed in the present investigation, are mobilized from their vascular stem cell niche after an acute myocardial infarction to restore blood perfusion to the damaged heart [Massa et al., 2009; Cheng et al., 2015]. Unfortunately, the amount of ECFCs that successfully engraft within the infarcted area is not sufficient to effectively restore local blood supply [Moccia et al., 2015; Tasev et al., 2016]. The intrinsic limitation of this endogenous reparative ability leads to the subsequent development of post-infarction heart failure, which represents one of the main causes of death, morbidity, and loss of life quality in industrialized countries [Steg et al., 2013]. The present investigation demonstrated for the first time that NAADP-containing liposomes may be successfully employed to

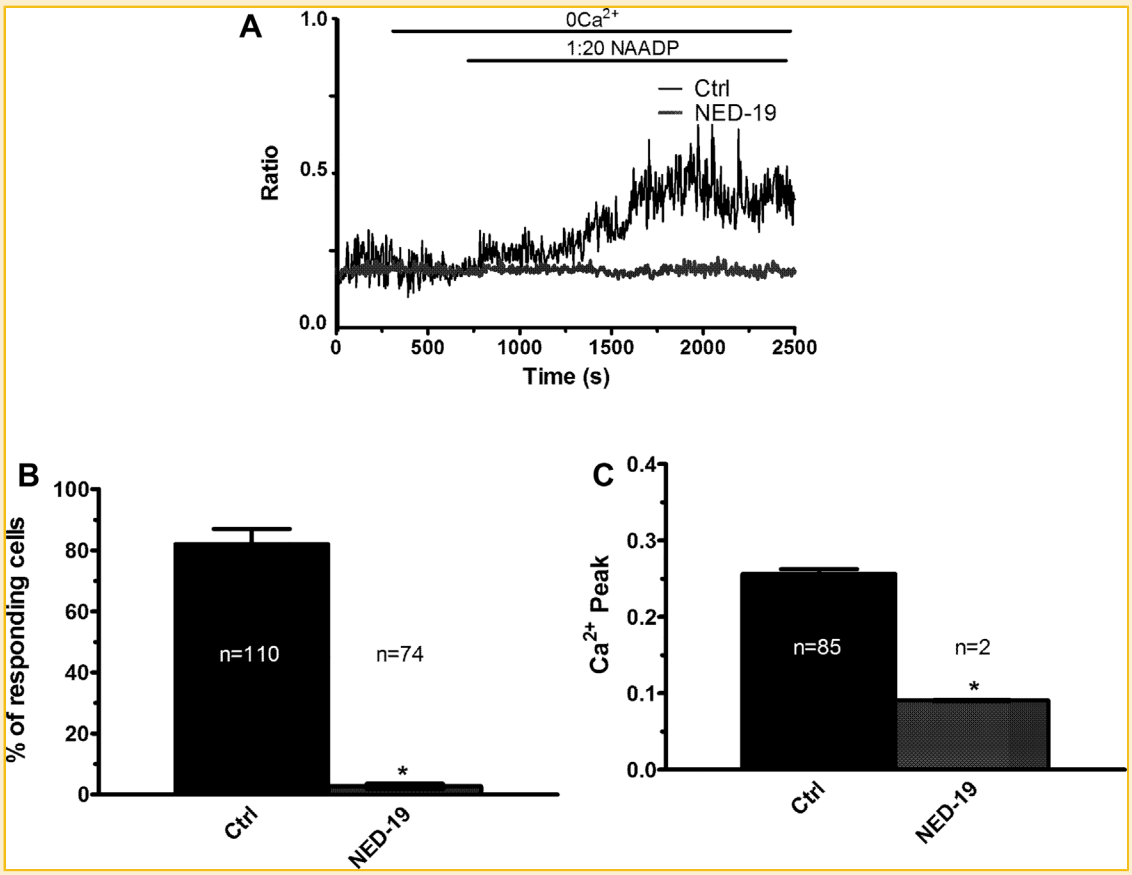

Fig. 5. The Ca^{2+} response to liposome-introduced NAADP is inhibited by NED-19. (A) NAADP in PL dispersions (1:20) increase $[Ca^{2+}]_i$ in the absence, but not the presence, of NED-19 (10 μM, 30 min). Mean ± SE of the percentage of responding cells (B) and of the magnitude (C) of NAADP-evoked Ca^{2+} signals in the absence and presence of NED-19. The asterisk indicates *t*-test *P*-value <0.05.

induce intracellular Ca^{2+} signaling and promote proliferation in ECFCs. This approach retains a significant therapeutic relevance as liposomes may be conferred a specificity toward a defined cell type.

Previous studies showed the intracellular levels of NAADP may be increased by using NAADP-encapsulating liposomes. In particular, NAADP-containing liposomes were exploited to stimulate neurite outgrowth in mouse neurons [Brailoiu et al., 2005] and neurotransmitter release at the frog neuromuscular junction [Brailoiu et al., 2003]. The formulations were prepared by dissolving NAADP within a KCl buffer. However, our preliminary experiments revealed that KLs did not cause any detectable increase in $[Ca^{2+}]_i$ in ECFCs. Of note, although the liposomes used in our experiments were composed of neutral lipids, each having one phosphatidyl group and one choline group in their molecules, they displayed a non-zero surface electric potential. One explanation for this observation is that an increase of ionic strength or temperature causes a structural change of the head-group region of the liposomes. As a result, lipid molecules could be arranged in such a way that the hydrophilic groups are located on the surface of liposomes under our conditions. This hypothesis could explain the failure of KLs in eliciting intracellular Ca^{2+} signaling despite the fact that the lipid composition of our vesicles is similar to that described by Brailoiu et al. [2003]. Accordingly, the surface charge was significantly higher in KLs as compared with PLs and it is well known that a large negative charge on a smaller liposome increases its surface charge and renders it impermeable to the cell membrane. Consistently, PLs induced a dose-dependent endogenous Ca^{2+} release, which was inhibited by NED-19, a selective blocker of NAADP signaling [Morgan et al., 2011; Ronco et al., 2015]. Preliminary experiments indicated that NAADP entry into the cells occurs by endocytosis (not shown). This finding, along with the observation that the NAADP-gated TPC1 is expressed in ECFCs [Zuccolo et al., 2016b], confirmed that PL formulations were suitable to load these cells with NAADP, thereby activating its prominent downstream signaling pathway, that is, intracellular Ca^{2+} mobilization. Of note, while the magnitude of the Ca^{2+} response to NAADP was higher at the lowest dilution tested (1:20), the percentage of responding cells increased by increasing NAADP dilution (1:30). One possible explanation for this observation is that TPC1 desensitizes at high NAADP concentrations [Morgan et al., 2011]. It could be that, at a higher dilution (1:30), liposomes release a sufficient amount of NAADP to activate most cells, although it is not enough to trigger the maximum Ca^{2+} release. Conversely, at 1:20 dilution the cytosolic NAADP concentration could attain such high levels to desensitize NAADP receptors in most

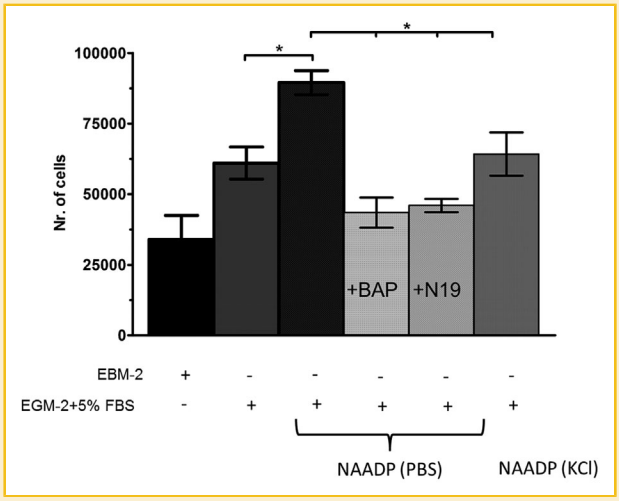

Fig. 6. Liposome-introduced NAADP stimulates ECFC proliferation. Number (mean ± SE) of ECFCs counted after 5 days in culture under the designated treatments. The asterisk indicates *t*-test *P*-value <0.05. Please, note that only PL dispersions (1:20) promoted ECFC proliferation and that this process was inhibited by pretreating the cells with BAPTA (BAP) (30 μM, 30 min) or NED-19 (N19) (10 μM; 30 min). KL dispersions were also used at 1:20 dilution.

cells while triggering the greatest Ca^{2+} mobilization in those escaping desensitization. Similar results have been obtained upon intracellular delivery of NAADP through a patch-pipette [Cancela et al., 1999] or through UV-induced photolysis of caged-NAADP [Moccia et al., 2006].

A recent study revealed that NAADP may be synthesized in response to vascular endothelial growth factor (VEGF) stimulation to promote proliferation in human umbilical vein endothelial cells (HUVEC) [Favia et al., 2014], a widely employed model to study endothelial cell functions in vitro. However, it was not clear yet whether NAADP per se was able to induce angiogenesis. This study showed that NAADP-containing liposomes stimulated ECFC proliferation by activating TPC1, as demonstrated by the inefficacy of such treatment in the presence of NED-19 or BAPTA, a fast exogenous Ca^{2+} buffer which is able to prevent the $[Ca^{2+}]_i$ to increase and recruit Ca^{2+}-dependent decoders. Therefore, in principle, liposomes could be used as a drug delivery system to load with NAADP ECFCs homing to the infarcted myocardium and boost the reparative process. Of course, this hypothesis remains to be probed in vivo by future research, but it is worth of noting that liposomes composed of negatively charged lipids supplemented with cholesterol are less prone to be removed from circulation and have already reached the pharmacological market [Senior, 1987]. Moreover, the lower surface charge of PLs used in the present investigation renders them considerably less toxic for the host [Immordino et al., 2006].

In conclusion, herein we described a novel method to prepare NAADP-containing liposomes to effectively induce ECFC proliferation in vitro by recruiting the Ca^{2+}-dependent mitogenic machinery. This strategy holds promise as an alternative maneuver to boost post-ischemic vascularization of infarcted hearts.

REFERENCES

Aihua Z, Qiang M, Quanguo H, Rong G, Chunwei Y. 2003. Interaction of malachite green with lecithin liposomes. Colloids Surf A: Physicochem Eng Asp 224:75–82.

Ambrosone L, Ceglie A, Colafemmina G, Palazzo G. 1999. Emulsions: A time-saving evaluation of the droplets' polydispersity and of the dispersed phase self-diffusion coefficient. Langmuir 15:6775–6780.

Basile DP, Yoder MC. 2014. Circulating and tissue resident endothelial progenitor cells. J Cell Physiol 229:10–16.

Brailoiu E, Hoard JL, Filipeanu CM, Brailoiu GC, Dun SL, Patel S, Dun NJ. 2005. Nicotinic acid adenine dinucleotide phosphate potentiates neurite outgrowth. J Biol Chem 280:5646–5650.

Brailoiu E, Patel S, Dun NJ. 2003. Modulation of spontaneous transmitter release from the frog neuromuscular junction by interacting intracellular Ca (2+) stores: Critical role for nicotinic acid-adenine dinucleotide phosphate (NAADP). Biochem J 373:313–318.

Bufalo G, Di Nezza F, Cimino L, Cuomo F, Ambrosone L. 2017. Physicochemical investigation of ultrasound effects on some steps of mink fur processing. A suggestion for improving the worker health and reducing the environmental impact. J Clean Prod 143:10–16.

Cancela JM, Charpentier G, Petersen OH. 2003. Co-ordination of Ca(2+) signalling in mammalian cells by the new Ca(2+)-releasing messenger NAADP. Pflugers Arch 446:322–327.

Cancela JM, Churchill GC, Galione A. 1999. Coordination of agonist-induced Ca2+-signalling patterns by NAADP in pancreatic acinar cells. Nature 398:74–76.

Cheng M, Huang K, Zhou J, Yan D, Tang YL, Zhao TC, Miller RJ, Kishore R, Losordo DW, Qin G. 2015. A critical role of Src family kinase in SDF-1/CXCR4-mediated bone-marrow progenitor cell recruitment to the ischemic heart. J Mol Cell Cardiol 81:49–53.

Dasa SS, Suzuki R, Gutknecht M, Brinton LT, Tian Y, Michaelsson E, Lindfors L, Klibanov AL, French BA, Kelly KA. 2015. Development of target-specific liposomes for delivering small molecule drugs after reperfused myocardial infarction. J Control Release 220:556–567.

Di Biasio L, Ambrosone L, Cametti C. 2009. Numerical simulation of dielectric spectra of aqueous suspensions of non-spherical differently shaped biological cells. J Phys D: Appl Phys 25401–25407:25401–25407.

Dragoni S, Reforgiato M, Zuccolo E, Poletto V, Lodola F, Ruffinatti FA, Bonetti E, Guerra G, Barosi G, Rosti V, Moccia F. 2015. Dysregulation of VEGF-induced proangiogenic Ca2+ oscillations in primary myelofibrosis-derived endothelial colony-forming cells. Exp Hematol 43:1019.e3–1030.e3.

Favia A, Desideri M, Gambara G, D'Alessio A, Ruas M, Esposito B, Del Bufalo D, Parrington J, Ziparo E, Palombi F, Galione A, Filippini A. 2014. VEGF-induced neoangiogenesis is mediated by NAADP and two-pore channel-2-dependent Ca2+ signaling. Proc Natl Acad Sci USA 111: E4706–E4715.

Ferreira-Martins J, Rondon-Clavo C, Tugal D, Korn JA, Rizzi R, Padin-Iruegas ME, Ottolenghi S, De Angelis A, Urbanek K, Ide-Iwata N, D'Amario D, Hosoda T, Leri A, Kajstura J, Anversa P, Rota M. 2009. Spontaneous calcium oscillations regulate human cardiac progenitor cell growth. Circ Res 105:764–774.

Galione A. 2015. A primer of NAADP-mediated Ca(2+) signalling: From sea urchin eggs to mammalian cells. Cell Calcium 58:27–47.

Galione A, Chuang KT, Funnell TM, Davis LC, Morgan AJ, Ruas M, Parrington J, Churchill GC. 2014. Synthesis of NAADP-AM as a membrane-permeant NAADP analog. Cold Spring Harb Protoc 2014:pdb.prot076927.

Gwathmey JK, Yerevanian AI, Hajjar RJ. 2011. Cardiac gene therapy with SERCA2a: From bench to bedside. J Mol Cell Cardiol 50:803–812.

Immordino ML, Dosio F, Cattel L. 2006. Stealth liposomes: Review of the basic science, rationale, and clinical applications, existing and potential. Int J Nanomedicine 1:297–315.

Ishi F, Takamura A, Ishigami I. 1995. Procedure for preparation of lipid vesicles (liposomes) using the coacervation (phase separation) technique. Langmuir 11:483–486.

Johnson JD, Misler S. 2002. Nicotinic acid-adenine dinucleotide phosphate-sensitive calcium stores initiate insulin signaling in human beta cells. Proc Natl Acad Sci USA 99:14566–14571.

Liu S, Levine SR, Winn HR. 2011. Targeting ischemic penumbra Part II: Selective drug delivery using liposome technologies. J Exp Stroke Transl Med 4:16–23.

Lopez F, Venditti F, Ambrosone L, Colafemmina G, Ceglie A, Palazzo G. 2004. Gelatin microemulsion-based gels with the cationic surfactant cetyltrimethylammonium bromide: A self-diffusion and conductivity study. Langmuir 20:9449–9452.

Massa M, Campanelli R, Bonetti E, Ferrario M, Marinoni B, Rosti V. 2009. Rapid and large increase of the frequency of circulating endothelial colony-forming cells (ECFCs) generating late outgrowth endothelial cells in patients with acute myocardial infarction. Exp Hematol 37:8–9.

Moccia F, Fotia V, Tancredi R, Della Porta MG, Rosti V, Bonetti E, Poletto V, Marchini S, Beltrame L, Gallizzi G, Da Prada GA, Pedrazzoli P, Riccardi A, Porta C, Zambelli A, D'Incalci M. 2017. Breast and renal cancer-derived endothelial colony forming cells share a common gene signature. Eur J Cancer. https://doi.org/10.1016/j.ejca.2017.01.025

Moccia F, Guerra G. 2016. Ca(2+) Signalling in endothelial progenitor cells: Friend or foe? J Cell Physiol 231:314–327.

Moccia F, Lim D, Nusco GA, Ercolano E, Santella L. 2003. NAADP activates a Ca2+ current that is dependent on F-actin cytoskeleton. FASEB J 17:1907–1909.

Moccia F, Lodola F, Dragoni S, Bonetti E, Bottino C, Guerra G, Laforenza U, Rosti V, Tanzi F. 2014. Ca2+ signalling in endothelial progenitor cells: A novel means to improve cell-based therapy and impair tumour vascularisation. Curr Vasc Pharmacol 12:87–105.

Moccia F, Nusco GA, Lim D, Kyozuka K, Santella L. 2006. NAADP and InsP3 play distinct roles at fertilization in starfish oocytes. Dev Biol 294:24–38.

Moccia F, Ruffinatti FA, Zuccolo E. 2015. Intracellular Ca(2)(+) signals to reconstruct a broken heart: Still a theoretical approach?. Curr Drug Targets 16:793–815.

Morgan AJ, Platt FM, Lloyd-Evans E, Galione A. 2011. Molecular mechanisms of endolysosomal Ca2+ signalling in health and disease. Biochem J 439:349–374.

Parkesh R, Lewis AM, Aley PK, Arredouani A, Rossi S, Tavares R, Vasudevan SR, Rosen D, Galione A, Dowden J, Churchill GC. 2008. Cell-permeant NAADP: A novel chemical tool enabling the study of Ca2+ signalling in intact cells. Cell Calcium 43:531–538.

Penny CJ, Kilpatrick BS, Eden ER, Patel S. 2015. Coupling acidic organelles with the ER through Ca(2)(+) microdomains at membrane contact sites. Cell Calcium 58:387–396.

Ronco V, Potenza DM, Denti F, Vullo S, Gagliano G, Tognolina M, Guerra G, Pinton P, Genazzani AA, Mapelli L, Lim D, Moccia F. 2015. A novel Ca(2)(+)-mediated cross-talk between endoplasmic reticulum and acidic organelles: Implications for NAADP-dependent Ca(2)(+) signalling. Cell Calcium 57:89–100.

Senior JH. 1987. Fate and behavior of liposomes in vivo: A review of controlling factors. Crit Rev Ther Drug Carrier Syst 3:123–193.

Steg PG, James SK, Gersh BJ. 2013. 2012 ESC STEMI guidelines and reperfusion therapy: Evidence-based recommendations, ensuring optimal patient management. Heart 99:1156–1157.

Tasev D, Koolwijk P, van Hinsbergh VW. 2016. Therapeutic potential of human-derived endothelial colony-forming cells in animal models. Tissue Eng Part B Rev 22:371–382.

Wolf IM, Diercks BP, Gattkowski E, Czarniak F, Kempski J, Werner R, Schetelig D, Mittrucker HW, Schumacher V, von Osten M, Lodygin D, Flugel A, Fliegert R, Guse AH. 2015. Frontrunners of T cell activation: Initial, localized Ca2+ signals mediated by NAADP and the type 1 ryanodine receptor. Sci Signal 8:ra102.

Zuccolo E, Bottino C, Diofano F, Poletto V, Codazzi AC, Mannarino S, Campanelli R, Fois G, Marseglia GL, Guerra G, Montagna D, Laforenza U, Rosti V, Massa M, Moccia F. 2016a. Constitutive store-operated Ca(2+) entry leads to enhanced nitric oxide production and proliferation in infantile hemangioma-derived endothelial colony-forming cells. Stem Cells Dev 25:301–319.

Zuccolo E, Dragoni S, Poletto V, Catarsi P, Guido D, Rappa A, Reforgiato M, Lodola F, Lim D, Rosti V, Guerra G, Moccia F. 2016b. Arachidonic acid-evoked Ca2+ signals promote nitric oxide release and proliferation in human endothelial colony forming cells. Vascul Pharmacol 87:159–171.

Zuccolo E, Lim D, Poletto V, Guerra G, Tanzi F, Rosti V, Moccia F. 2015. Acidic Ca2+ stores interact with the endoplasmic reticulum to shape intracellular Ca2+ signals in human endothelial progenitor cells. Vascul Pharmacol 75:70–71.